Virology 526 (2019) 1–12

Contents lists available at ScienceDirect

Virology

journal homepage: www.elsevier.com/locate/virology

Role of c-Jun terminal kinase (JNK) activation in influenza A virus-induced autophagy and replication

Jingting Zhang[a,1], Tao Ruan[a,1], Tianyu Sheng[a], Jiongjiong Wang[a], Jing Sun[a,b], Jin Wang[d], Richard A. Prinz[e], Daxin Peng[c,f], Xiufan Liu[c,f], Xiulong Xu[a,b,f,*]

[a] College of Veterinary Medicine, Yangzhou University, Yangzhou 225009, Jiangsu Province, PR China
[b] Institute of Comparative Medicine, Yangzhou University, Yangzhou 225009, Jiangsu Province, PR China
[c] Animal Infectious Disease Laboratory, College of Veterinary Medicine, Yangzhou University, Yangzhou 225009, China
[d] Center for Immunological Research, Houston Methodist Research Institute, Houston, TX 77030, USA
[e] Department of Surgery, NorthShore University Health System, Evanston IL60201, USA
[f] Jiangsu Co-innovation Center for Prevention and Control of Important Animal Infectious Diseases and Zoonosis, Yangzhou University, Yangzhou 225009, Jiangsu Province, PR China

ARTICLE INFO

Keywords:
Influenza A virus
Autophagy
NS1
JNK
PI-3 kinase

ABSTRACT

The non-structural protein 1 (NS1) of different influenza A virus (IAV) strains can differentially regulate the activity of c-Jun terminal kinase (JNK) and PI-3 kinase (PI3K). Whether varying JNK and PI3K activation impacts autophagy and IAV replication differently remains uncertain. Here we report that H5N1 (A/mallard/Huadong/S/2005) influenza A virus induced functional autophagy, as evidenced by increased LC3 lipidation and decreased p62 levels, and the presence of autolysosomes in chicken fibroblast cells. H9N2 (A/chicken/Shanghai/F/98) virus weakly induced autophagy, whereas H1N1 virus (A/PR/8/34, PR8) blocked autophagic flux. H5N1 virus activated JNK but inhibited the PI-3 kinase pathway. In contrast, N9N2 virus infection led to modest JNK activation and strong PI-3 kinase activation; whereas H1N1 virus activated the PI-3 kinase pathway but did not activate JNK. SP600125, a JNK inhibitor, inhibited H5N1 virus-induced autophagy and virus replication in a DF-1 chicken fibroblast cell line. Our study uncovered a previously unrecognized role of JNK in IAV replication and autophagy.

1. Introduction

Autophagy is a catabolic process that mediates the degradation of damaged organelles, unneeded proteins, and invading microbes (Galluzzi et al., 2014; Russell et al., 2014). Based on how substrates are delivered to lysosomes, autophagy is classified into three major subtypes: chaperone-mediated autophagy, microautophagy, and macroautophagy (Galluzzi et al., 2014; Russell et al., 2014). In chaperone-mediated autophagy, cytosolic substrate proteins, which contain a consensus pentapeptide motif (KEERQ) and can be recognized by chaperone heat shock cognate (HSC70), are sequestered into the lysosomal lumen by interacting with lysosome-associated membrane protein type 2 (LAMP2) (Galluzzi et al., 2014; Russell et al., 2014) Microautophagy involves the direct engulfment of cytoplasmic cargo by an autophagic tube, which forms by invagination of the lysosomal membrane and undergoes vesicle scission into the lysosomal lumen (Dong and Levine, 2013; Galluzzi et al., 2014; Russell et al., 2014; Steele et al., 2015). Macroautophagy (hereafter referred as autophagy) begins by the initial formation of a crescent-shaped double-membrane known as the isolation membrane or phagophore (Galluzzi et al., 2014; Russell et al., 2014). The phagophore subsequently elongates and, upon the fusion of the phagophore edge, encloses the cytoplasmic material to form autophagosome (Galluzzi et al., 2014; Russell et al., 2014). Autophagosomes finally mature into organelles and then fuse with lysosomes to form autolysosomes where lysosomal enzymes digest the autophagosome content as well as the inner autophagosome membrane (Galluzzi et al., 2014; Russell et al., 2014).

Autophagy is initiated by the activation of VPS34, a Class III PI-3 kinase in the preinitiation complex, which contains several other proteins, including Beclin-1, ATG14L, and VPS15 (Dumit and Dengjel, 2012; Galluzzi et al., 2014; Russell et al., 2014). VPS34 is activated by UNC-51-like kinase 1 (ULK1), a serine/threonine kinase that interacts

* Corresponding author at: College of Veterinary Medicine, Yangzhou University, Yangzhou 225009, Jiangsu Province, PR China.
E-mail address: xxl@yzu.edu.cn (X. Xu).
[1] These authors contributed equally.

https://doi.org/10.1016/j.virol.2018.09.020
Received 31 August 2018; Received in revised form 25 September 2018; Accepted 25 September 2018
Available online 10 October 2018
0042-6822/

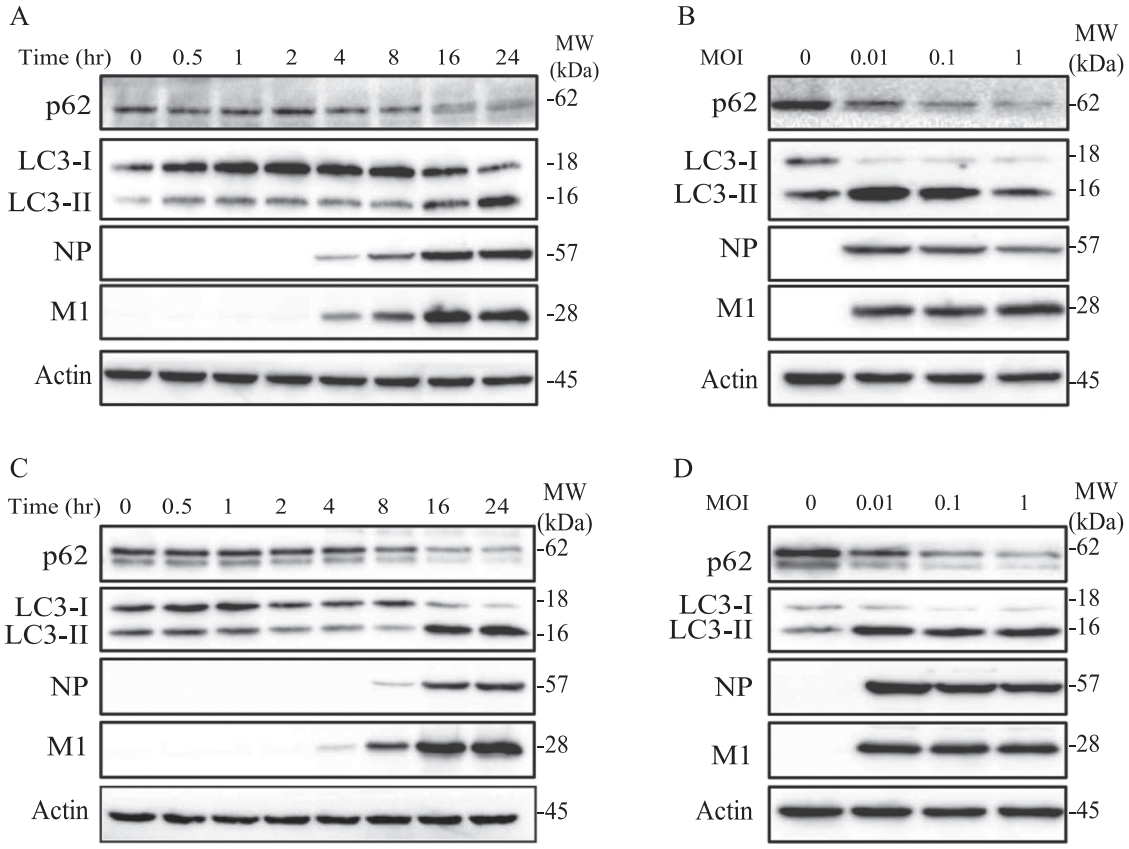

Fig. 1. IAV induces LC-3 lipidation and p62 degradation in CEF and DF-1 cells. CEF (**A & B**) and DF1 cells (**C & D**) were infected with 0.1 MOI of H5N1 virus and incubated for the indicated time (**A & C**) or with the indicated MOI (0, 001, 0.1, and 1) for 24 h (**B & D**). Cell lysates were prepared and analyzed for LC3-II lipidation and the levels of p62, NP, M1, and β-actin by Western blot.

with ATG13 and FIP200. Once activated, this pre-initiation complex catalyzes phosphatidylinositol (PI)-4,5 to PI 3-phosphate (PI3P), a phospholipid involved in the elongation and nucleation of the double membrane, to form autophagosomes (Dumit and Dengjel, 2012; Galluzzi et al., 2014; Russell et al., 2014). ULK1 activity is regulated by the mechanistic target of rapamycin (mTOR) and AMP-activated protein kinase (AMPK), two nutrient- and energy-sensitive kinases, respectively (Mack et al., 2012; Shang et al., 2011). These two kinases phosphorylate ULK1 at different serine residues and have the opposite effect on ULK activity: mTOR phosphorylates ULK1 at serine 757 ($ULK1^{S757}$) and inhibits its activity; whereas AMPK phosphorylates ULK1 at multiple sites, including the serine residues 317, 555, and 777 ($ULK1^{S317/S555/S717}$), and activates it (Bach et al., 2011; Kim et al., 2011). c-Jun terminal kinase (JNK), a stress-activated protein kinase, regulates autophagy by phosphorylating Bcl-2 and releasing its binding from Beclin-1 (Wei et al., 2008a, 2008b). Beclin-1 becomes available for the formation of the preinitiation complex (Wei et al., 2008a, 2008b). Alternatively, Beclin-1 can be phosphorylated by AMPK and freed from the Bcl-2-Beclin-1 complex (Kim et al., 2013; Zhang et al., 2016a).

Influenza A virus (IAV) infects a wide range of avian and mammalian hosts, whereas influenza B virus primarily infects humans (Hsu, 2018). IAV can be further classified into various subtypes based on the combination of two viral surface glycoproteins, e.g., hemagglutinin (HA) and neuraminidase (NA) (Hsu, 2018). A total of 18 HA and 11 NA subtypes have been identified so far. Among them, several reassortant IAV genotypes, including H5N1, H9N2, H7N2, and H6N5, cause sporadic fatal infections in humans (Hsu, 2018; Lai et al., 2016). Although numerous studies have shown that IAV is able to induce autophagy, many issues remain to be solved (Dumit and Dengjel, 2012; Zhang et al., 2014). For example, how IAV infection triggers the initiation of autophagy is not clear; the role of autophagy in IAV replication remains controversial; whether IAV subtypes can differentially induce functional autophagy has not been thoroughly investigated.

The non-structural protein (NS1) of influenza A virus binds multiple cellular proteins and plays important roles in regulating apoptosis, antiviral immunity, and virus replication (Hsu, 2018; Klemm et al., 2018; Krug, 2015). In particular, the NS1 protein of H1N1 and H3N2 viruses binds to the p85 β subunit of PI-3 kinase and activates its enzymatic activity (Ehrhardt and Ludwig, 2009; Ehrhardt et al., 2006, 2007a, 2007b; Hale et al., 2008, 2006; Li et al., 2008; Shin et al., 2007a, 2007b). It has been suggested that AKT activation in the PI-3 kinase pathway can suppress JNK activation (Lu et al., 2010). Other IAV subtypes such as H5N1 virus are unable to activate the PI-3 kinase pathway (Li et al., 2012) but can activate JNK (Nacken et al., 2014). JNK activation is required for autophagy induced by several types of virus such as hepatitis B virus (Zhong et al., 2017), oncolytic adenovirus (Klein et al., 2015), and Sendai virus (Siddiqui and Malathi, 2012). In the present study, we compared the ability of three different subtypes of IAV, including H5H1, H9N2, and H1N1 viruses, to regulate the PI-3 kinase pathway and to activate JNK. We found that H5N1 virus induced functional autophagy by activating JNK and suppressing the PI-3 kinase pathway. In contrast, H1N1 virus activated the PI-3 kinase pathway but did not activate JNK, whereas H9N2 virus activated both the PI-3 kinase pathway and JNK. H1N1 and H9N2 viruses induced incomplete autophagy.

2. Results

2.1. H5N1 virus induces functional autophagy in CEF

Most studies investigating the ability of IAV to induce autophagy have been carried out in mammalian tumor cell lines, which usually have abnormal autophagy. Here we tested if the H5N1 virus (A/mallard/Huadong/S/2005), an IAV subtype that primarily infects poultry and replicates well in avian cells, was able to induce autophagy in primary CEF and the DF1 chicken fibroblast cell line. As shown in Fig. 1, H5N1 virus infection increased LC3-II lipidation and decreased p62 levels in CEF (Fig. 1A & B) and DF1 (Fig. 1C & D) in a time- (Fig. 1A & C) and dose-dependent manner (Fig. 1B & D). At the dose of 0.1 multiplicity of infection (MOI), increased LC3-II lipidation became remarkable post-inoculation at 16 and 24 h, whereas p62 degradation was visible starting at 4 and 8 h post inoculation. The infection dose as low as 0.1 MOI was able to dramatically increase LC3-II lipidation and decrease p62 levels in both CEF and DF1 cells 24 h post-inoculation. Viral M1 and NP protein synthesis was detected at 4 and 8 h post inoculation, which corresponded to the time points when p62 protein was degraded.

2.2. Opposite effect of different IAV subtypes on autophagy

We next determined if three different IAV strains (H5N1, A/mallard/Huadong/S/2005; H9N2, A/Ck/SH/F/98; H1N1, A/PR8/34), each with two different doses, could differentially induce autophagy in CEF. H5N1 virus was used at 0.01 and 0.1 MOI, whereas H9N2 and H1N1 viruses were used at 0.1 and 1 MOI for infection of CEF. The reason for different doses of these three IAV subtypes is that H5N1 virus, an avian IAV subtype, generally replicates faster in CEF than two other subtypes. As shown in Fig. 2A, H5N1 virus at 0.01 and 0.1 MOI dramatically increased LC3-II lipidation and decreased p62 levels. H9N2 virus at 0.1 and 1 MOI modestly increased LC3-II lipidation but did not decrease p62 levels. In contrast, H1N1 virus at 0.1 and 1 MOI dramatically increased p62 levels and modestly increased the LC3-II/LC3-I ratio. Of note, the M1 expression levels of three IAV subtypes were almost equal, indicating that the difference in autophagy induction by these three IAV subtypes are not due to differing virus replication rates. These observations suggest that H5N1 virus induces functional autophagy, H1N1 virus did not induce functional autophagy but rather arrested the autophagic flux.

We next conducted confocal microscopy to determine if three different IAV strains also differentially induced the formation of autophagosomes. As shown in Fig. 2B, H5N1 virus induced the formation of autophagic puncta which distributed perinuclearly. The puncta distribution was similar to those in a positive control in rapamycin-treated DF-1 cells. In contrast, H1N1 virus-induced autophagosomes form very large-size puncta that concentrated on one side near the nuclei. H9N2 virus-induced puncta mostly scattered on one side near the nuclei. All three IAV subtypes induced the formation of autophagosomes in approximately 30% of GFP-positive DF1 cells (Fig. 2C). Rapamycin included as a positive control gave rise to approximately 15% autophagosome-positive cells (Fig. 2C).

To verify the ability of H5N1 virus to induce functional autophagy, we tested if blocking the autophagic flux by chloroquine (CQ), a lysosomal protease inhibitor, and bafilomycin A, an H-ATPase inhibitor, could affect the levels of LC3-II lipidation and p62 expression. CQ (2 μM) and bafilomycin A (10 nM) itself had no effect on p62 levels but increased the levels of LC3-II and the ratios of LC3-II to LC-I in uninfected cells (Fig. 3A & B). CQ and bafilomycin A enhanced H5N1 virus-induced LC3-II lipidation and partially blocked H5N1 virus-induced p62 degradation (Fig. 3A). In contrast, CQ and bafilomycin A had almost no effect on p62 levels and LC3 lipidation in H1N1 virus-infected cells. The ability of H5N1 virus to induce functional autophagy was further verified by confocal microscopy of DF-1 cells in the presence of bafilomycin A. As shown in Fig. 3C, bafilomycin A (10 nM) or H5N1 virus (0.1 MOI) significantly increased the formation of autophagsomes as the number of GFP-LC3 puncta was significantly increased in uninfected DF-1 cells. Bafilomycin A plus H5N1 virus further increased the number of GFP-LC3 puncta in H5N1-infected cells (Fig. 3D).

We next determined if inhibition of autophagy affected IAV replication. As shown in Fig. 3E, bafilomycin A dramatically decreased the levels of NP and M1 proteins in the conditioned media and cell lysates in H5N1-infected CEF, and lowered the virus titers in the conditioned media of H5N1-infected CEF. Bafilomycin A only slightly decreased the levels of NP and M1 proteins in the conditioned media and the cell lysates of H1N1 virus-infected CEF and slightly decreased the virus titer in the conditioned media in H1N1-infected CEF (Fig. 3H). Bafilomycin A slightly but significantly decreased cell proliferation in uninfected CEF but did not further decrease the proliferation of H5N1 virus-infected cells (Fig. 3G).

The ability of three IAV subtypes to differentially induce the formation of autolysosomes was further verified by using DF-1 cells stably expressing GFP-RFP-LC3. The green fluorescence of GFP is quenched in the acidic environment in autolysosomes, whereas the red fluorescence of RFP is illuminated in autolysosomes. Autophagosomes illuminate as the orange puncta through the combination of red and green fluorescence. As shown in Fig. 4A, there were very few puncta (7.05 ± 0.19/cell) in the uninfected cells. There were significantly more autophagosomes present perinuclearly in the cytoplasm in H5N1 virus-infected cells. The mean number of puncta per cell in H5N1-infected DF-1 cells was 40.3 ± 0.66. Among them, 65.5 ± 0.9% of the puncta illuminated with red RFP fluorescence (Fig. 4B), which represent autolysosomes. In contrast, approximately 80% puncta were illuminated with orange fluorescence in H9N2 and H1N1 virus-infected DF-1 cells, which represent autophagosomes. These observations further suggest that H5N1 virus induces functional autophagy, whereas H9N2 and H1N1 viruses block autophagic flux in DF-1 cells.

2.3. The PI-3 kinase pathway is differentially activated by three IAV subtypes

We next determined if autophagy induced by three IAV subtypes correlated with the activation of the PI-3 kinase pathway. As shown in Fig. 5A, AKT^{S473} and $mTOR^{S2448}$ phosphorylation was transiently increased between 8 and 16 h post-inoculation (hpi) but inhibited at 24 hpi in H5N1 virus-infected CEF. Interestingly, phosphorylation of $S6K1^{T389}$ and $ULK1^{S757}$, two substrates of mTOR, was not changed in the early stage of infection before 8 hpi but was decreased in the late stage at 16–18 hpi. AKT^{S473}, $mTOR^{T\ 2448}$, and $ULK1^{S757}$ phosphorylation dramatically decreased 24 hpi in CEF infected with as low as 0.01 MOI H5N1 virus (Fig. 5B). Of note, total ULK1 of chicken origin was not detectable due to the lack of reactivity of commercially available antibodies. β-actin was used as a loading control.

We next compared the ability of three IAV subtypes to regulate the PI-3 kinase pathway. Again, AKT^{S473}, $S6K1^{T389}$, and $ULK1^{S757}$ phosphorylation was decreased in CEF infected with H5N1 virus at 0.01 and 0.1 MOI but was weakly increased in CEF infected with H1N1 virus at 0.1 and 1 MOI at 24 hpi. In contrast, H9N2 virus infection at 0.1 and 1 MOI dramatically increased AKT^{S473} and $S6K1^{T389}$ phosphorylation but unexpectedly decreased $ULK1^{S757}$ phosphorylation. It is not clear if decreased $ULK1^{S757}$ phosphorylation in H9N2 virus-infected cells was due to the decrease of total ULK1 protein, which could be caused by ubiquitination-induced degradation or by inhibition of protein synthesis. Therefore, the PI-3 kinase pathway was differentially regulated by these three IAV subtypes, leading to different autophagy outcomes.

2.4. Differential activation of JNK by three IAV subtypes

JNK is implicated in regulating autophagy by disrupting Bcl-2 and Beclin-1 interaction (Wei et al., 2008a, 2008b). Here we tested if JNK

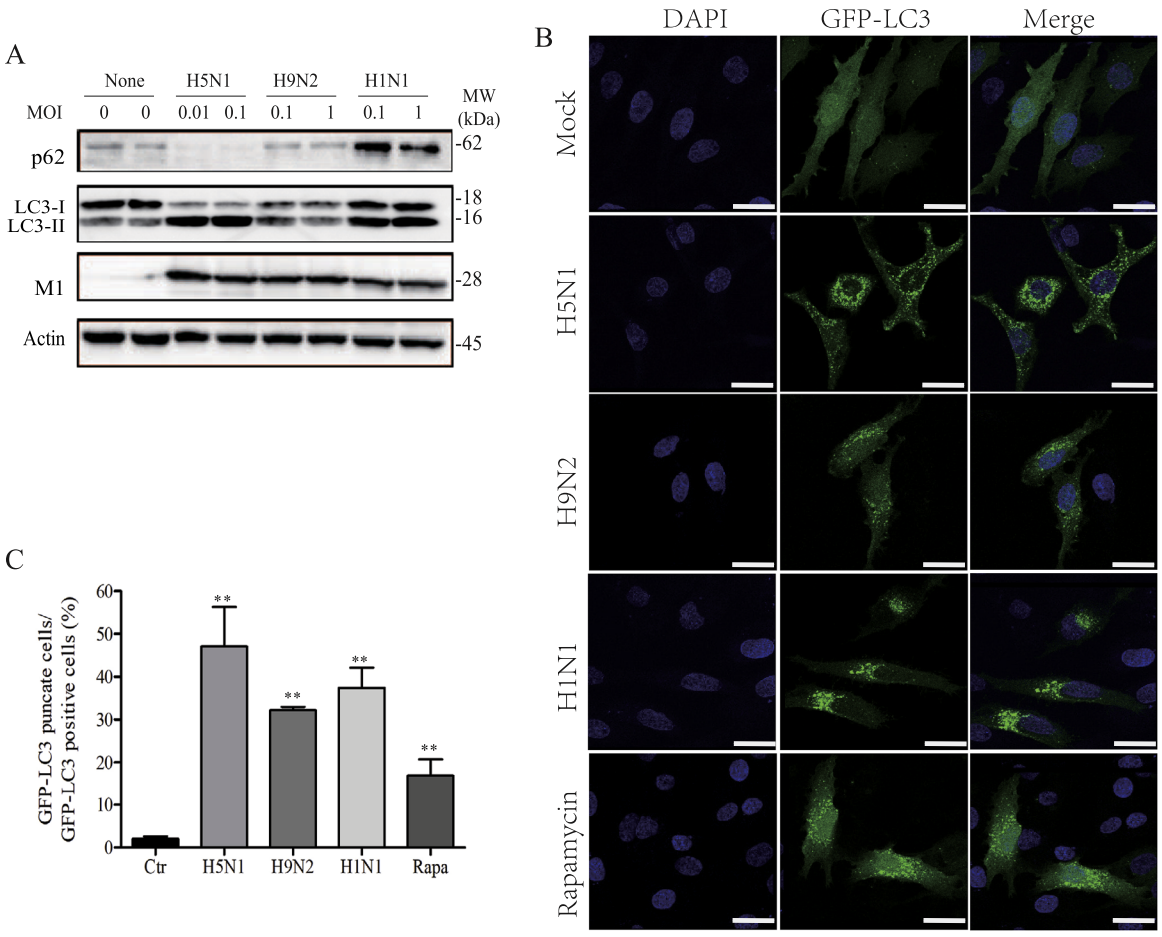

Fig. 2. Differential autophagy induction by three IAV subtypes. (A) CEF were infected with the indicated MOI of three IAV subtypes (H5N1, H9N2, and H1N1) for 24 h. Cell lysates were analyzed for LC3-II lipidation and the levels of p62, M1, and β-actin expression by Western blot. (**B**) DF-1 cells were transiently transfected with the expression vector pmLC3-GFP. The cells were left infected or infected with H5N1 (0.1 MOI), H9N2 (1 MOI) or H1N1 (1 MOI). Uninfected cells treated with rapamycin (50 nM) were included as a positive control. After incubation for 12 h, autophagosomes were visualized under a confocal microscope. Scale bar, 25 μm. The percent of the cells with the presence of autophagosomes among the GFP-positive DF-1 cells was calculated and plotted in a bar graph with statistical analysis (**C**). $**p < 0.01$, compared to untreated control.

was differentially activated by three IAV subtypes and correlated with their ability to induce functional autophagy. As shown in Fig. 6A, H5N1 virus infection of CEF with 0.1 MOI induced JNK and Beclin-1 phosphorylation at 8–24 hpi in a time-dependent manner. H5N1 virus infection of CEF with various doses of MOI (0.01, 0, 1, and 1) dramatically increased JNK phosphorylation and modestly increased Beclin-1 phosphorylation at 24 hpi (Fig. 6B). Similar observations were made with DF-1 cells (Fig. 6C & D). We then compared the ability of three IAV subtypes to activate JNK and Beclin-1. H5N1 virus at 0.01 and 0.1 MOI remarkably increased JNK and Beclin-1 phosphorylation, H9N2 modestly increased JNK phosphorylation and weakly increased Beclin-1 phosphorylation; whereas H1N1 virus almost had no effect on JNK and Beclin-1 phosphorylation (Fig. 6E).

Finally, we determined if JNK activation was required for H5N1 virus-induced autophagy and virus replication. As shown in Fig. 7A, SP600125, a specific inhibitor of JNK, blocked H5N1 virus-induced LC3-II lipidation and p62 degradation. Consistently, SP600125 blocked H5N1 virus-induced autophagosome formation (Fig. 7B & C). Moreover, SP600125 lowered the titer of H5N1 virus in the conditioned media and the cytoplasmic fraction of DF1 cells in a dose-dependent manner (Fig. 7D & E). Inhibition of virus replication by SP600125 was not due to its inhibitory effect on DF-1 cell proliferation since SP600125 inhibited DF-1 proliferation marginally (Fig. 7F). These observations suggest that JNK may enhance H5N1 virus replication by inducing autophagy.

3. Discussion

In the present study, we provide unambiguous evidence that a strain of H5N1 subtype of IAV induced functional autophagy in CEF, whereas H9N2 and H1N1 subtypes induced incomplete autophagy. Differences in autophagy induced by these different IAV subtypes were due to alternative activation of JNK and the PI-3 kinase pathways. We further showed that autophagy was inhibited by bafilomycin A or by a JNK inhibitor, leading to suppression of H5N1 virus replication. Our study is the first to suggest that JNK activation enhances IAV replication by promoting autophagy.

IAV induces the accumulation of autophagosomes in various mammalian cell lines in vitro and in mouse and human lung tissues in vivo. For example, the H1N1 WSN strain induces autophagy in MDCK cells; H5N1 (A/Jilin/9/2004) and H1N1 (A/new.Coledonia/20/1999) viruses induce autophagy in A549 cells (Zhou et al., 2009). Zhirnov and Klenk (2013) reported that H1N1 PR8 strain induces the formation of autophagosomes in MDCK cells. Autophagy induction was evidenced by increased LC3-II lipidation and the perinuclear presence of autophagosome puncta (Zhirnov and Klenk, 2013; Zhou et al., 2009). Whether p62 was degraded by these viruses was not investigated in these two studies (Zhirnov and Klenk, 2013; Zhou et al., 2009). It is not clear if these IAV subtypes indeed induced functional autophagy or induced the accumulation of autophagosomes by blocking the autophagic flux (Zhirnov and Klenk, 2013; Zhou et al., 2009). Pan et al. (2014) reported

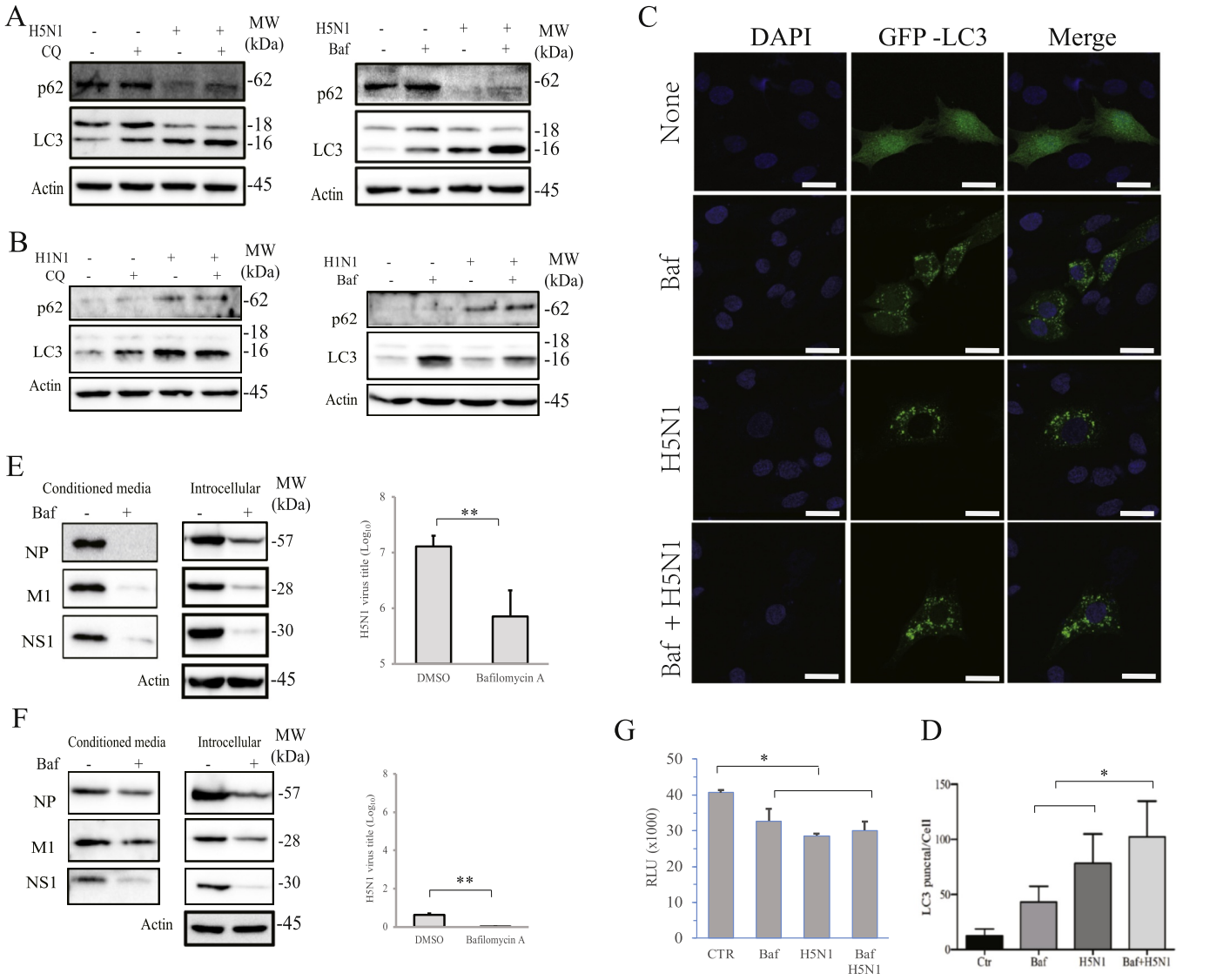

Fig. 3. Effect of bafilomycin A and CQ on IAV-induced LC-3 lipidation and p62 degradation. (**A & B**) CEF were left uninfected or infected with H5N1 (1 MOI) (**A**) or H1N1 (10 MOI) viruses (**B**). After incubation for 12 h, chloroquine (2 μM) or bafilomycin A (Baf) (10 nM) was added and incubated for another 8 h. Cell lysates were analyzed for p62, LC3, and β-actin expression by Western blot. (**C**) DF-1 cells transfected with the pmLC3-GFP expression vector was left uninfected or infected with H5N1 virus (5 MOI). After incubation for 12 h, bafilomycin A (10 nM) was added and incubated for another 8 h. Autophagosomes were visualized under a confocal microscope. Scale bar, 25 μm. The number of puncta per cell was calculated and plotted in a bar graph with statistical analysis (D). $*p < 0.05$, compared to the number of puncta in the cells treated with bafilomycin A or with H5N1 virus infection. (**E-F**) Effect of bafilomycin A on virus replication and cell proliferation. CEF were inoculated with H5N1 (0.1 MOI) (E) or H1N1 (1 MOI) viruses (**F**) and then incubated in the absence or presence of bafilomycin A (10 nM) for 24 h. Cell lysates were prepared for the levels of NP and M1 viral protein expression. The conditioned media collected and analyzed for the TCID50 values. (**G**) Effect of bafilomycin A on CEF proliferation. CEF seeded in 96-well plates were left uninfected or infected with IAV H5N1 virus (0.1 MOI) and then incubated in the absence or presence of bafilomycin A (10 nM) for 24 h, followed by cell proliferation assay as described in Materials and Methods. Data are the mean ± SD of the triplicate from one representative of three experiments with similar results. $*p < 0.05$, compared to untreated control.

that H5N1 pseudotyped particles induced autophagy in A549 cells, by observing p62 protein degradation. In the present study, we compared the ability of three IAV subtypes, H5N1, H9N2, and H1N1, to induce autophagy in CEF. Our results showed that the H5N1 virus induced functional autophagy, as evidenced by increased LC3-II lipidation and decreased p62 levels. Furthermore, the H5N1 virus induced the formation of autolysosomes, as evidenced by the presence of increased number of RFP-LC3 puncta surrounding the nuclei and the presence of red fluorescent puncta in RFP-GFP-LC3-infected CEF. These observations collectively suggest that the H5N1 virus induces complete and functional autophagy. In contrast, the H1N1 virus induced accumulation of autophagosomes, as evidenced by increased LC3-II lipidation and lack of p62 degradation. Confocal microscopy revealed that RFP-LC3 and GFP-LC3 fluorescent puncta were almost always co-localized in H9N2 and H1N1 virus-infected CEF. These observations collectively suggest that H1N1 viruses block autophagic flux, leading to the formation of autophagosomes but not the formation of autolysosomes. Of note, the differential autophagy induced by H5N1, H9N2 or H1N1 viruses was not due to the differential infectivity and replication rates of these viruses in CEF since two different MOIs for each subtype were used to ensure equal or similar levels of viral protein synthesis.

The mechanisms by which H1N1 virus blocks the autophagic flux were independently investigated by several laboratories. Gannage et al. (2009) reported earlier that H1N1 virus (A/PR8) blocks the fusion of autophagosomes with lysosomes through the interaction of its M2 protein with Beclin-1, thus inhibiting the autophagosome flux.

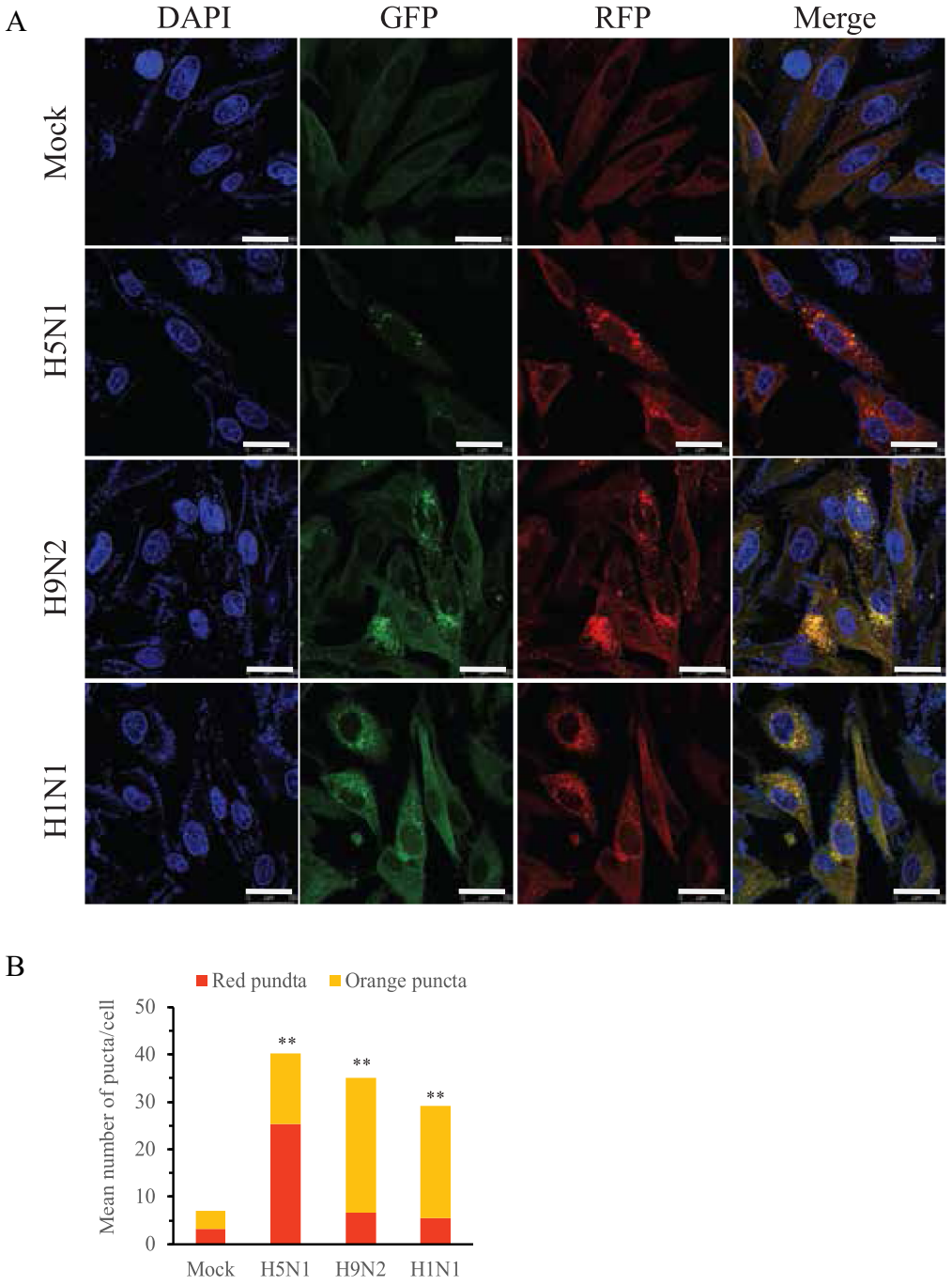

Fig. 4. H5N1 but not H9N2 and H1N1 viruses induce the formation of autolysosomes. DF-1 cells stably expressing the GFP-RFP-LC3 gene were left uninfected or infected with H5N1 (1 MOI), H9N1 (5 MOI) or H1N1 (5 MOI) for 12 h. The cells were then fixed and stained with DAPI. Autophagosomes presented as the orange puncta and autolysosomes presented as the red puncta were visualized under a confocal microscope (**A**). Scale bar, 25 μm. (**B**) The numbers of red and orange puncta per cell were plotted in a bar graph. * *$p < 0.01$, the number of orange and red puncta in IAV-infected DF-1 cells compared to that in a mock-infected control.

Inhibition of M2 expression through M2 siRNA or infection with M2-deficient PR8 virus prevents the accumulation of autophagosomes. Further studies by these authors suggest that the proton channel activity is not required for the inhibition of the formation of autolysosomes. In contrast, Ren et al. (2015) reported that the proton channel activity of M2 protein of H3N2 virus (A/Hong Kong/8/68) is required for the blockade of the autophagosome-lysosome fusion. The M2 channel inhibitor amantadine is able to block the inhibitory effect of M2 protein on autolysosome formation; Whereas the mutant M2 protein that lacks this channel activity fails to block autophagosome-lysosome fusion (Ren et al., 2015). Beale et al. (2014) showed that the M2 protein of the PR8 virus interacts with LC3 and is required for LC3 membrane translocation, filamentous budding, and virus stability. Our present study showed that H1N1 and H9N2 viruses arrested the autophagic flux, as evidenced by increased p62 levels (Fig. 2A) and the absence of autolysosomes (Fig. 4). In contrast, the H5N1 virus did not block autophagic flux but rather induced functional autophagy in CEF and DF-1 cells. The amino acid sequence in the highly conserved LC3-interacting region (LIR) of the M2 protein of the H5N1 virus is FVNI (He et al., 2013), which is slightly different from that in the H1NI virus with a FVSI motif (Beale et al., 2014). Beale et al. (2014) reported that the FVNI motif in the M2 protein of the H5N1 virus has a higher affinity

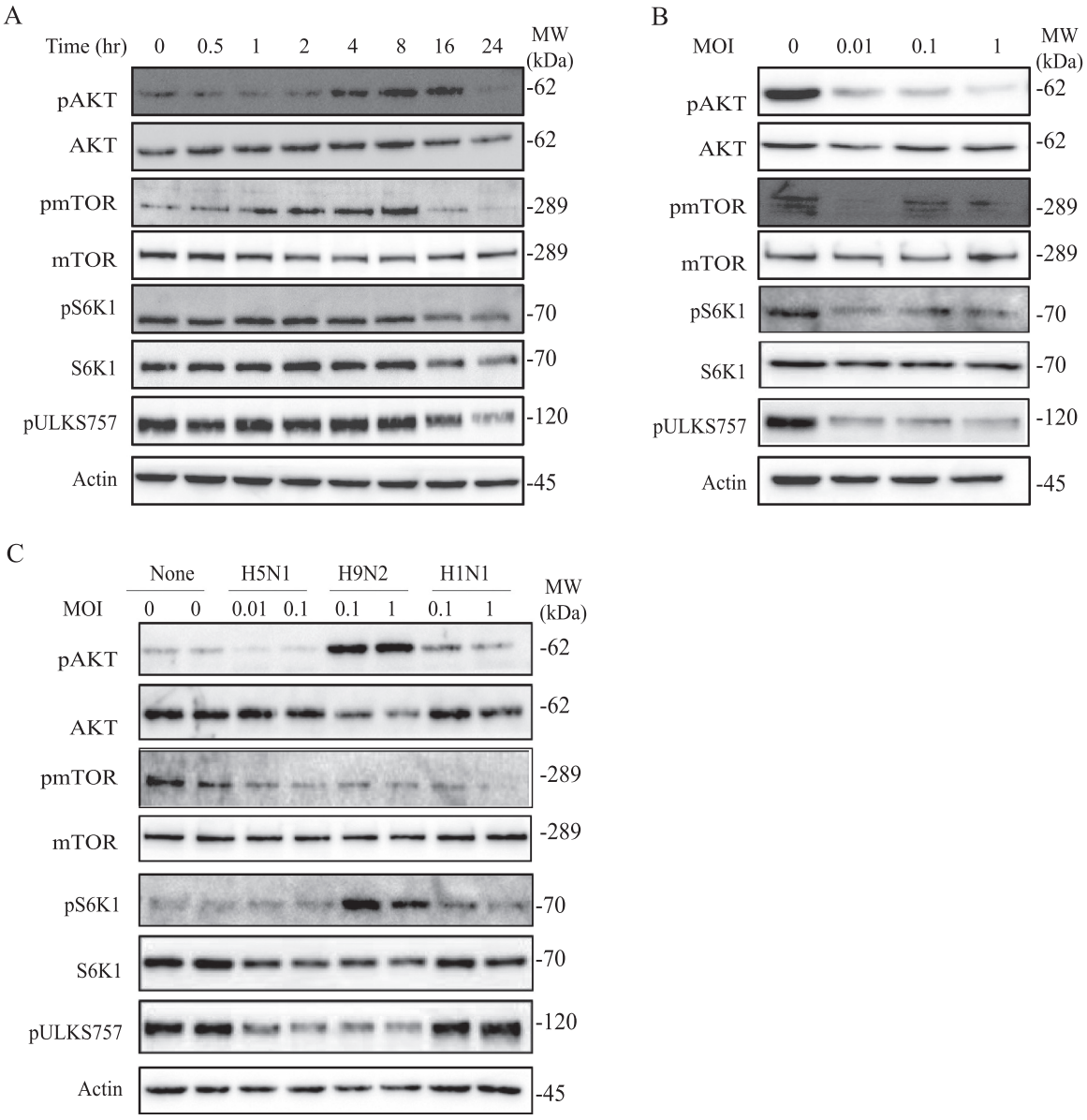

Fig. 5. Effect of IAV infection on the PI-3 kinase pathway. CEF were inoculated with 0.1 MOI of the H5N1 virus and incubated for the indicated time (**A**) or inoculated with the indicated MOI of the H5N1 virus for 24 h (**B**). Cell lysates were analyzed for the levels of phosphorylation and total proteins by Western blot with the indicated antibodies. (**C**) CEF infected with the indicated MOI of the three IAV subtypes for 24 h. Cell lysates were analyzed for the levels of phosphorylation and total proteins by Western blot with the indicated antibodies.

toward LC3 than the FVSI in the M2 protein of the H1N1 virus. In addition, the A/mallard/Huadong/S/2005 H5N1 strain at the amino acid position 86 has a valine (He et al., 2013) versus an alanine in the PR8 H1N1 strain (Beale et al., 2014). This should further enhance the binding of the M2 protein of this H5N1 strain to LC3. It remains puzzling why the H5N1 virus was unable to arrest autophagy but rather induced functional autophagy in CEF and DF-1 cells (Fig. 7 G).

Although it is well established that certain IAV subtypes such as the H1N1 virus arrest autophagic flux (Beale et al., 2014; Gannage et al., 2009; Munz, 2014; Ren et al., 2015; Rossman and Lamb, 2009), whether the autophagic process has a role in IAV replication remains controversial (Steele et al., 2015). Zhou et al. (2009) reported earlier that inhibition of autophagy by 3-methylademine (3-MA), wortmannin, Beclin-1 or LC3 siRNA leads to the inhibition of H1N1 virus (A/WSN/33 strain) replication in Madin-Darby canine kidney (MDCK) cells, as evidenced by decreased viral RNA and virus titers. Similarly, Liu et al. (2016) reported that H1N1 viruses (A/WSN/33 & A/PR8/34) replicate significantly slower in ATG7-deficient murine embryonic fibroblast (MEF) cells, as evidenced by decreased synthesis of viral proteins and RNAs. Yeganeh et al. (2015) reported that bafilomycin A at the concentrations ranging from 0.1 to 100 nM inhibits the replication of IAV (A/PR/8/34) in A549 cells, and that bafilomycin A at 10–100 nM blocks autophagic flux. Hahn et al. (2014) reported that a 50% reduction of ATG5 expression in alveolar epithelial cells leads to a significant reduction of replication of the HKx31 strain of the H3N2 virus. In contrast, Gannage et al. (2009) reported that wild-type MEF cells retain more viral RNA and proteins of an H3N2 virus (A/Aichi/68) than ATG5-deficient MEF cells, and that there is no significant difference in virus titers in the supernatants of wild-type and ATG5-deficient MEF cells. Sun et al. (2012) reported that inhibition of autophagy by ATG5 siRNA and 3-MA in A549 cells and in the lungs of mice did not change the titers of H5N1 virus (A/Jilin/9/2004), albeit 3-MA or ATG4 siRNA treatment significantly prolongs the survival of mice infected with H5N1 virus. It is not clear if different effects of autophagy on virus replication were due to the different cell lines used in these studies. Our present study showed that bafilomycin A dramatically reduced viral

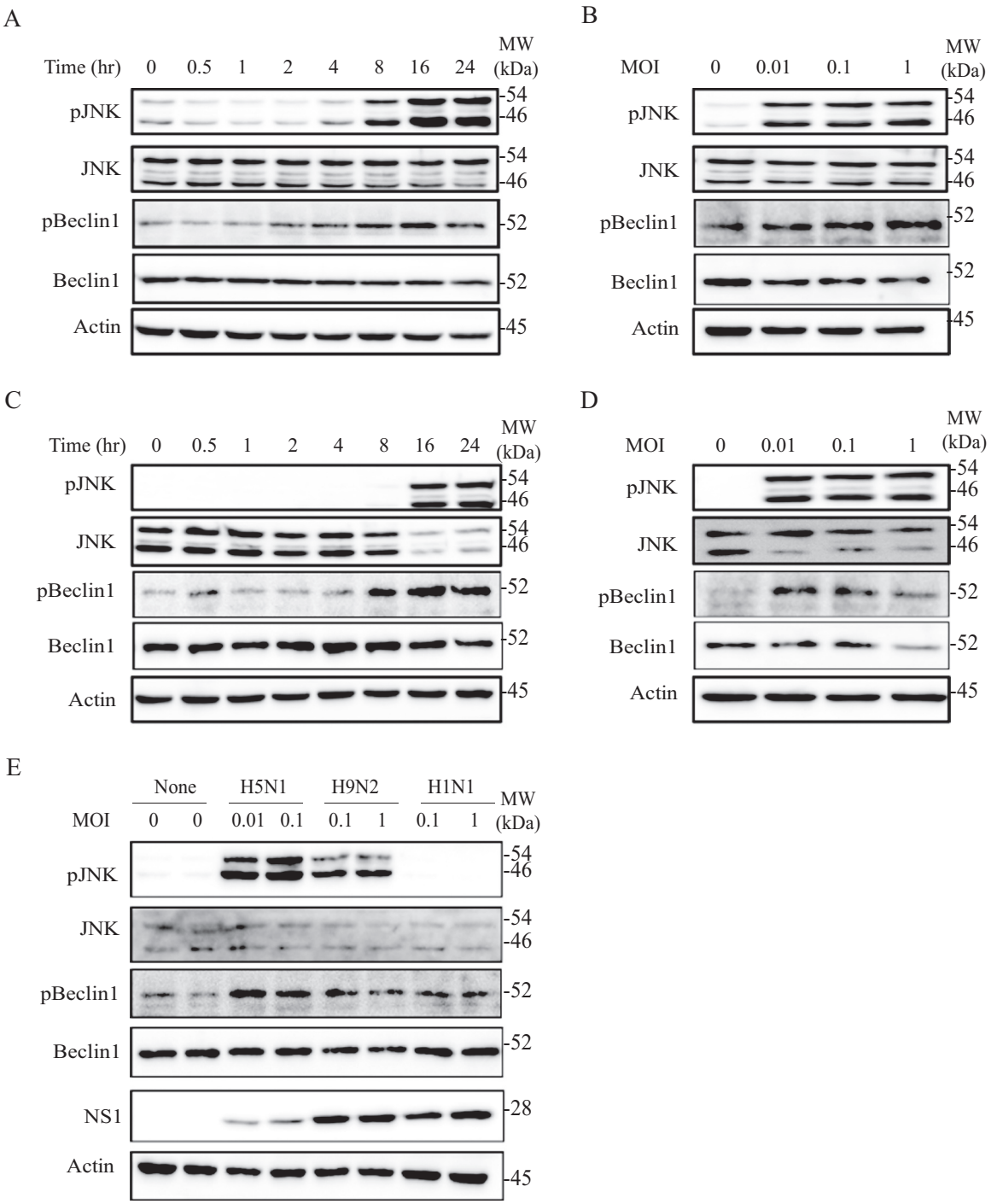

Fig. 6. Effect of IAV infection on JNK activation. CEF (**A & B**) and DF1 cells (**C & D**) were infected with 0.1 MOI of the H5N1 virus and incubated for the indicated time (**A & C**) or inoculated with the indicated MOI of theH5N1 virus for 24 h (**B & D**). Cell lysates were analyzed for JNK and Beclin-1 phosphorylation and their total protein levels by Western blot with the indicated antibodies. (**E**) CEF were infected with the indicated MOI of the three IAV subtypes for 24 h. Cell lysates were analyzed for JNK and Beclin-1 phosphorylation and their total protein levels by Western blot with the indicated antibodies.

protein synthesis and decreased the titer of H5N1 virus in CEF but marginally inhibited H1N1 viral protein synthesis. Weak inhibition of H1N1 virus replication by bafilomycin could be due to incomplete blockade of the autophagic flux since H1N1 virus slightly increased the number of red puncta in DF-1 cells (Fig. 4).

Different IAV strains can differentially activate JNK. Ludwig et al. (2001) first reported that JNK is rapidly activated by some IAV subtypes such as avian A/Bratislava/79 (H7N9) and human IAV A/Asia/579 (H2N2) viruses. Interestingly, a widely used PR8 strain, an H1N1 virus, blocks virus replication-induced JNK activation (Ludwig et al., 2002). Later studies revealed that in addition to viral RNA, the NS1 protein of IAV with a phenylalanine at position 103 of its amino acid sequence is required for JNK activation (Nacken et al., 2014). PR8 is a unique IAV strain. It has a serine residue at the 103 position in its NS1 protein; whereas most other IAV strains have a phenylalanine residue at the 103 position (Nacken et al., 2014). Sequence analysis revealed F103 in the NS1 gene of both H9N2 (Zhang et al., 2008) and H5N1 viruses (He et al., 2013). H9N2 and H5N1 viruses readily induced JNK phosphorylation and activation. However, the mechanism by which the NS1 protein of IAV activates JNK remains to be resolved.

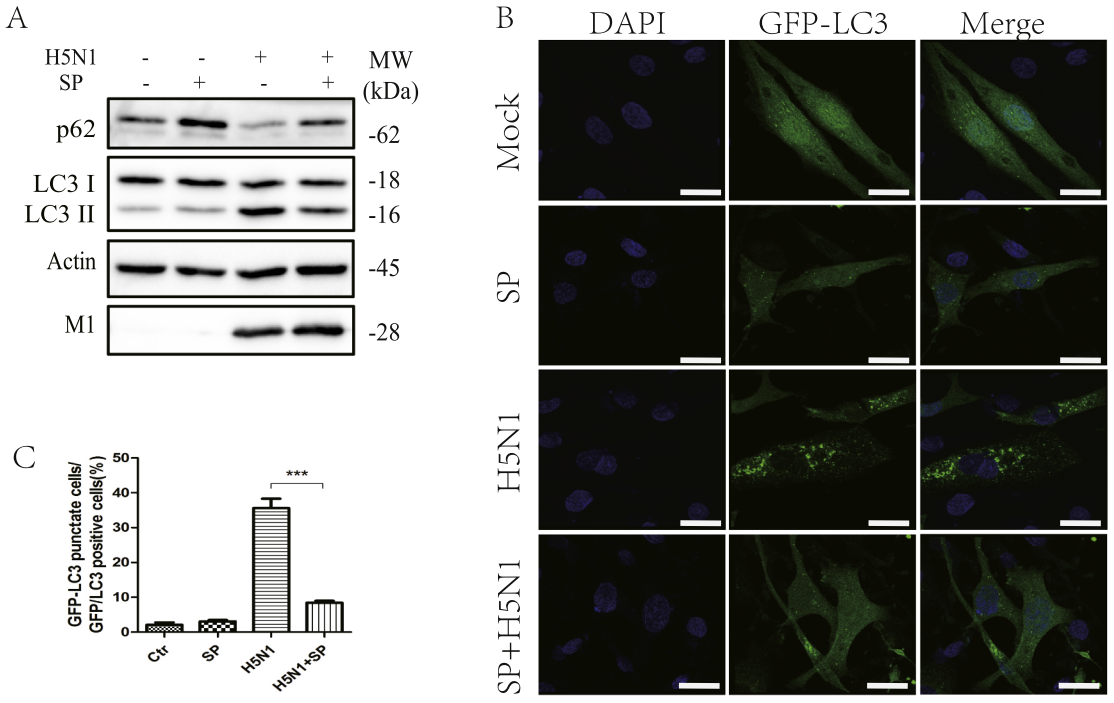

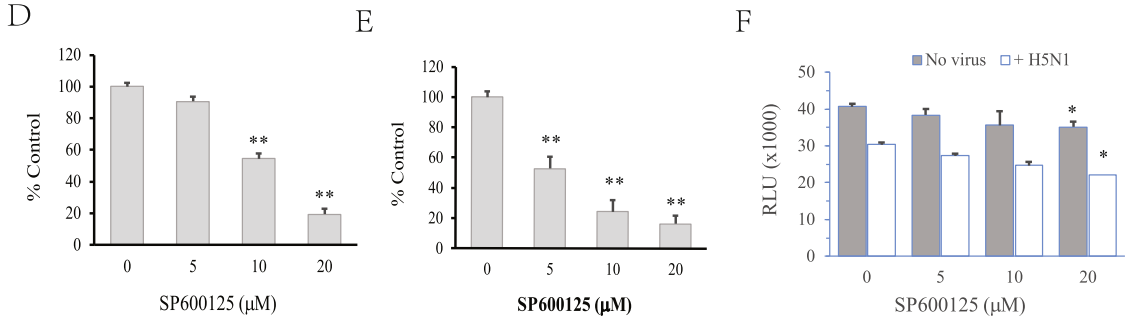

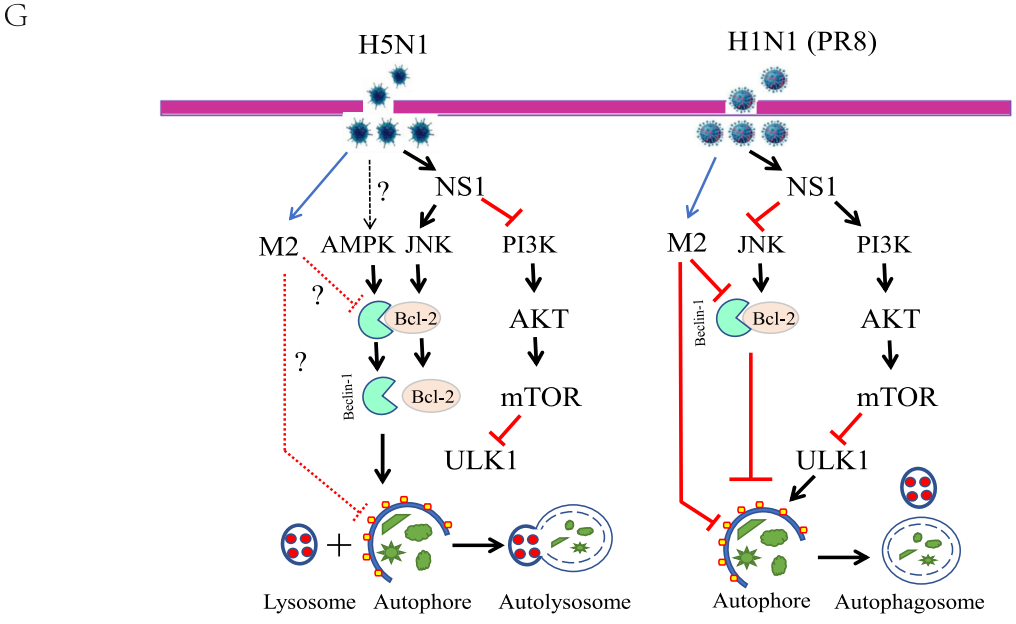

(caption on next page)

Fig. 7. Effect of JNK inhibition on IAV-induced autophagy and virus replication. (**A**) Effect of SP600125 on IAV-induced autophagy. DF-1 cells were inoculated with the H5N1 virus (0.1 MOI) and then incubated in the absence or presence of SP600125 (10 μM) for 24 h. The cell lysates were analyzed for LC3-II lipidation, p62, M1 expression, and β-actin. (**B**) Effect of SP6000125 on IAV-induced autophagosome formation. DF-1 cells were transiently transfected with the expression vector pmLC3-GFP. After incubation for 36 h, the cells left uninfected or infected with the H5N1 virus (5 MOI) in the absence or presence of SP600125 (10 μM) for 12 h. Autophagosomes were visualized under a confocal microscope. Scale bar, 25 μm. The percent of the cells with the presence of autophagosomes among the entire GFP-positive DF-1 cells were calculated and plotted in a bar graph with statistical analysis (**C**). (**D**) Effect of SP600125 on IAV replication. CEF were inoculated with the H5N1 virus (0.1 MOI) and then incubated in the absence or presence of SP600125 (5, 10, 20 μM) for 24 h. Viral titers in the conditioned media (**D**) and cell lysates (**E**) were analyzed for the TCID50 values and subsequently converted into the percent of control. $**p < 0.01$, compared to untreated control. (**F**) Effect of SP600125 on DF-1 cell proliferation. DF-1 cells seeded in 96-well plates were left uninfected or infected with H5N1 virus (0.1 MOI) and incubated in the absence or presence of various concentrations of SP600125 (5, 10, 20 μM) for 24 h. Cell proliferation was analyzed as described in Materials and Methods. Data are the mean ± SD of the triplicate from one representative of three experiments with similar results. $*p < 0.05$, compared to uninfected or H5N1 virus-infected controls. (**G**) Schematic mode of IAV-induced autophagy. H5N1 virus enters cells through endocytosis via its α2,3-linked -sialic acid receptor. In addition to viral RNA, the NS1 protein of H5N1 virus activates JNK, phosphorylates Bcl-2, and disrupts its interaction with Beclin-1. Alternatively, Beclin-1 is released from the Bcl-2/Beclin-1 complex through its phosphorylation by AMPK, an energy-sensitive kinase activated by increased AMP levels at the late stage of virus replication or by other mechanisms. Once Beclin-1 becomes available, it is assembled into the pre-initiation complex, which contains several other proteins, including ATG14L, VSP15, and VPS34, a Class III PI-3 kinase activated by ULK1. ULK1 activity is suppressed by mTOR-mediated phosphorylation at S757 but activated by AMPK-mediated phosphorylation at S555, S317, and S777. The NS1 protein of H5N1 virus activated JNK and but inhibited the PI-3 kinase pathway. In contrast, the NS1 protein of H1N1 virus (PR8 strain) blocked JNK activation but activated the PI-3 kinase pathway, subsequently activating mTOR, inhibiting ULK1 activity and autophagy. It is not clear if AMPK is activated by PR8 virus, leading to $ULK1^{S555}$ phosphorylation and the suppression of mTOR activity. The M2 protein of IAV can interact with Beclin-1 and LC3. Inhibition of autophagic flux may lead to the accumulation of autophagosomes in H1N1 virus-infected cells. It remains unclear why the M2 protein of H5N1 virus did not block the formation of autolysosomes.

JNK activation has been implicated in playing an important role in autophagy. Wei et al. (2008a, 2008b) reported that JNK1 phosphorylates Bcl-2 at T69, S70, and S87 under nutrient starvation condition. Bcl-2 phosphorylation releases Beclin1 from the Bcl-2/Beclin1 complex, initiating starvation-induced autophagy (Wei et al., 2008a, 2008b). JNK activation is also involved in regulating virus-induced autophagy. For example, JNK activation in oncolytic adenovirus-infected cells leads to Bcl-2 phosphorylation and dissociation with Beclin-1 (Klein et al., 2015) and plays a critical role in autophagy induction mediated by oncolytic adenovirus (Klein et al., 2015), Sendai virus (Siddiqui and Malathi, 2012), the X protein of hepatitis B virus (Zhong et al., 2017), and cytosine-phosphate-guanine (CpG) (Wu et al., 2016). Our present study showed that the H5N1 virus induced JNK activation and autophagy, whereas the H1N1 virus did not activate JNK and did not induce the functional autophagy. Inhibition of JNK activation by a specific JNK inhibitor blocked H5N1 virus-induced autophagy. These observations collectively suggest that JNK activation plays a critical role in inducing complete autophagy.

In addition to regulating autophagy, JNK activation by IAV also plays an important role in apoptosis (Herold et al., 2012; Iwai et al., 2013; Ludwig et al., 2006), IFN-β production (Xie et al., 2014), and virus replication (Hrincius et al., 2010; Nacken et al., 2012; Xie et al., 2014; Zhang et al., 2016b). Down-regulation of the expression of c-Jun, a transcription factor of JNK, by a DNAzyme in vitro in human A549 cells and in vivo in mice by intranasal administration suppresses H5N1 virus replication. SP600125, a specific inhibitor of JNK, inhibits H5N1 and H7N7 virus replication in A549 cells and in the lungs of H7N7 and H1N1 virus-infected mice (Nacken et al., 2012; Zhang et al., 2016b). Consistent with these observations, our present studies showed that SP600125 inhibited H5N1 virus replication. The mechanism by which JNK activation enhances virus replication is not clear. Since JNK activation can induce apoptosis and stimulate anti-viral IFN-β production (Herold et al., 2012; Iwai et al., 2013; Ludwig et al., 2006), inhibition of JNK activity should have increased IAV replication. Instead, SP600125 suppressed IAV replication, suggesting that JNK activation enhances virus replication independent of its role in apoptosis and anti-viral immunity. Based on the observations that autophagy enhanced virus replication, and that inhibition of JNK activity suppressed autophagy and IAV replication, we propose that JNK stimulates IAV production by inducing autophagy. Although it is not clear how JNK activation-mediated autophagy benefits IAV replication, we speculate that autophagy may suppress virus replication in part by suppressing anti-viral immunity. This supposition is supported by evidence from recent studies showing that autophagy does down-regulate the expression of IFN and IFN-stimulated genes (Lindqvist et al., 2018; Perot et al., 2018). In addition, autophagy due to JNK activation may provide additional nutritional support for virus replication (Steele et al., 2015).

mTOR suppresses autophagy by phosphorylating $ULK1^{S757}$, which inhibits its activity. mTOR is activated in H1N1 virus-infected cells through its NS1 protein interaction with the p85 β subunit of PI-3 kinase. Our present study showed that H1N1 virus significantly increased AKT phosphorylation but only weakly increased $ULK1^{S757}$ phosphorylation (Fig. 5C). Similarly, Zhirnov and Klenk (2013) reported earlier that significant AKT activation did not lead to a remarkable increase of S6K1 phosphorylation. It is not clear if poor $ULK1^{S757}$ and $S6K1^{T398}$ phosphorylation in H1N1 virus-infected cells is due to the suppression of mTOR activity by activated AMPK. In contrast to H1N1 PR8 strain, the H5N1 virus did not activate the PI-3 kinase pathway in CEF. Instead, H5N1 virus infection of CEF led to the inhibition of the PI-3 kinase pathway and suppression of $ULK1^{S757}$ phosphorylation in the late stage of virus replication. These observations suggest that induction of H5N1 virus-induced autophagy may be in part due to inhibition of $ULK1^{S757}$ phosphorylation and ULK1 activation (Fig. 7G).

Due to the lack of reactivity of several commercial antibodies with the proteins of avian origins, our study has several limitations. Firstly, it is not clear if JNK activation leads to increased Bcl-2 phosphorylation and increased interaction with Beclin-1; Secondly, it is not clear if increased Beclin-1 phosphorylation is due to increased AMPK phosphorylation and activation in CEF. AMPK phosphorylation was increased in H5N1 virus-infected MDCK cells (Zhang et al, unpublished observations). Thirdly, the role of JNK in regulating autophagy and virus replication has not been further tested by using JNK siRNA or other genetic approaches. In addition, several critical questions remain. For instance, why the H5N1 virus whose M2 protein possesses a motif that should interact with LC3 did not prevent the formation of autolysosomes; whether JNK activation plays a role in ameliorating the blockade of autolysosome formation is not known; how H1N1 virus initiates the formation of autophagosomes remains unclear.

In summary, our present study provides clear evidence that the H5N1 virus induces complete and functional autophagy, whereas the H1N1 PR8 virus induces incomplete autophagy due to the blockade of autophagic flux. We further showed that JNK activation in CEF plays a critical role in H5N1 virus-induced autophagy and virus replication. Our study is the first to suggest that JNK activation regulates virus replication by inducing autophagy.

4. Materials and methods

4.1. Reagents

SP600125 was purchased from Cell Signaling Technology (Danvers, MA). Rapamycin was purchased from Cayman Laboratories (Ann Arbor, MI). Bafilomycin and chloroquine (CQ) were purchased from Sigma (St. Louis, MO). Anti-β-actin mAb was purchased from Santa Cruz Biotechnology, Inc. (Santa Cruz, CA). Antibodies against p62, Beclin-1, LC3, AKT, S6K1, and their corresponding phospho-antibodies including Beclin-1^{S93}, ULK1^{S757}, mTOR^{S2448}, AKT^{S473}, and S6K1^{T389} were purchased from Cell Signaling Technology (Danvers, MA). The expression vector encoding RFP-LC3 (pmRFP-LC3) was purchased from OriGene Technologies, Inc. (Rockville, MD). DF-1 cells were purchased from the American Tissue Culture Collection (Manassas, VA) and grown in complete DMEM medium supplemented with 10% fetal bovine serum, streptomycin and penicillin, and L-glutamine. Monoclonal or polyclonal antibodies against NP, M1, and HA proteins were prepared by immunizing mice with purified recombinant proteins.

4.2. Cell culture and viruses

Chicken embryo fibroblasts (CEF) were prepared and grown in M199 containing 4% fetal bovine serum. The A/mallard/Huadong/S/2005 H5N1 virus was isolated from poultry (He et al., 2013). Viruses were plaque purified three times in MDCK cells. A human influenza virus (A/PR8/34) was kindly provided by Dr. Liqian Zhu (College of Veterinary Medicine, Yangzhou University). IAV H9N2 virus (AIV Ck/SH/F/98) has been reported previously (Zhang et al., 2008). All IAV strains were propagated in 10-day-old specific-pathogen-free embryonic chicken eggs. The virus titers were measured by a 10-fold serial dilution (10^1 to 10^9, and each dilution (10^5 –10^9) inoculated into CEF cells. The 50% tissue culture infection dose ($TCID_{50}$/ml) was calculated according to the Reed and Muench method.

4.3. Virus growth

CEF cells infected with 0.1 MOI H5N1 virus were incubated with indicated concentrations of inhibitors for the indicated times. The $TCID_{50}$ values were determined according to our previous publications (He et al., 2013; Zhang et al., 2008). Data represent the mean ± standard deviation (SD) of 4 independent experiments.

4.4. Cell proliferation assay

To determine if the inhibitory effect of bafilomycin A and SP600125 on virus replication was due to its inhibitory effect on cell proliferation, DF-1 cells seeded in 96-well plates (2000 cells/well) were left uninfected or infected with 0.1 MOI H5N1 virus and then incubated in the absence or presence of indicated concentrations of bafilomycin A or SP600125. After incubation for 24 h, cell proliferation was analyzed by using an ATP-based Cell-Glo assay (Promegan, Madison, WI) following the manufacturer's instruction.

4.5. Autophagosome analysis

DF-1 cells stably transfected with pmLC3-GFP were seeded on coverslips and infected with H5N1 (1 MOI), H9N2 (5 MOI) or H1N1 (5 MOI) viruses. After incubation for 12 h, the cells were fixed in 4% paraformaldehyde at RT for 10 min and then stained for their nucleus in PBS containing 4,6-diamidino-2-phenylindole (0.5 μg/ml; Sigma Chemical Co.). The coverslips were mounted in PBS containing 50% glycerol. Autophagosomes were examined under a Leica LP8 confocal microscope. The green-colored puncta in the cells of ten random fields (100X) were counted in a blinded fashion. Results represent the mean puncta per cell ± SD (standard deviation) from one of three independent experiments with similar results. To determine the specificity of the H5N1 virus to induce functional autophagy, DF-1 cells stably transfected with pmLC3-GFP were infected with H5N1 virus (1 MOI) and then incubated in the absence or presence of bafilomycin A (10 nM) for 12 h. The cells were then fixed and analyzed for the presence of autophagosomes. To determine if JNK activation was required for H5N1 virus-induced autophagy, DF-1 cells stably transfected with pmLC3-GFP were infected with this virus (1 MOI) and then incubated in the absence or presence of SP600125 (10 μM), a specific inhibitor of JNK, for 12 h. The cells were then fixed and analyzed for the presence of autophagosomes.

4.6. Autolysosome analysis

DF-1 cells stably transfected with GFP-RFP-LC3 were similarly infected with the three IAV subtypes and analyzed for autolysosomes under a Leica LP8 confocal microscope. The red and orange puncta, which represent autolysosmes and autophagosomes, respectively, in the cells of ten random fields (100X) were counted in a blinded fashion. Results represent the mean puncta per cell ± SD (standard deviation) from one of three independent experiments with similar results. Percent red puncta = the number of red puncta ÷ (the number of red puncta + the number of orange puncta) x 100%.

4.7. Western blotting

CEF and DF-1 cells seeded in 6-well plates were infected with H5N1 (0.1 MOI), H1N1 or H9N2 viruses (1 MOI each) and then incubated in the absence or presence of various concentrations of inhibitors. Cells were harvested and lysed in NP-40 lysis buffer [50 mM Tris-HCl, pH 8.0, 150 mM NaCl, 1% NP-40, 5 mM EDTA, 5 mm EGTA, 1 mM NaF, 2 mM sodium vanadate, the cocktail of protease inhibitors (1X) (Pierce Chemical Co., Rockford, IL), 2 mM sodium pervandate]. Cell lysates were prepared and analyzed for the expression of viral proteins (HA, NP, and M1) or other indicated proteins (β-actin) with their specific antibodies, followed by horseradish peroxidase-conjugated goat anti-rabbit IgG and SuperSignal Western Pico enhanced chemiluminoscence substrate (Pierce Chemical Co., Rockford, IL). β-actin was detected as a loading control.

4.8. Statistical analysis

Differences in the virus titers in the conditioned media of virus-infected cells, in viral mRNA levels, and in cell proliferation were statistically analyzed by using an unpaired Student *t*-test. A p value of < 0.05 was considered statistically significant. All statistics were performed with SigmaPlot 11 software (Systat Software, Inc, San Jose, CA).

Acknowledgements

This work was supported in part by a start-up fund from the College of Veterinary Medicine, Yangzhou University, and the Priority Academic Program Development of Jiangsu Higher Education Institutions to Xiulong Xu, and by China Postdoctoral Science Foundation (2015M581873), Natural Science Foundation of Jiangsu Province (BK20150450), and the Scientific Research Foundation for the Returned Overseas Chinese Scholars, State Education Ministry (2015311) to Jing Sun. We are very grateful to Dr. Liqian Zhu for kindly providing H1N1 virus.

Conflict of interest

All authors declare no competing interest.

References

Bach, M., Larance, M., James, D.E., Ramm, G., 2011. The serine/threonine kinase ULK1 is a target of multiple phosphorylation events. Biochem. J. 440, 283–291.

Beale, R., Wise, H., Stuart, A., Ravenhill, B.J., Digard, P., Randow, F., 2014. A LC3-interacting motif in the influenza A virus M2 protein is required to subvert autophagy and maintain virion stability. Cell Host Microbe 15, 239–247.

Dong, X., Levine, B., 2013. Autophagy and viruses: adversaries or allies? J. Innate Immun. 5, 480–493.

Dumit, V.I., Dengjel, J., 2012. Autophagosomal protein dynamics and influenza virus infection. Front. Immunol. 3, 43.

Ehrhardt, C., Ludwig, S., 2009. A new player in a deadly game: influenza viruses and the PI3K/Akt signalling pathway. Cell. Microbiol. 11, 863–871.

Ehrhardt, C., Marjuki, H., Wolff, T., Nurnberg, B., Planz, O., Pleschka, S., Ludwig, S., 2006. Bivalent role of the phosphatidylinositol-3-kinase (PI3K) during influenza virus infection and host cell defence. Cell. Microbiol. 8, 1336–1348.

Ehrhardt, C., Wolff, T., Ludwig, S., 2007a. Activation of phosphatidylinositol 3-kinase signaling by the nonstructural NS1 protein is not conserved among type A and B influenza viruses. J. Virol. 81, 12097–12100.

Ehrhardt, C., Wolff, T., Pleschka, S., Planz, O., Beermann, W., Bode, J.G., Schmolke, M., Ludwig, S., 2007b. Influenza A virus NS1 protein activates the PI3K/Akt pathway to mediate antiapoptotic signaling responses. J. Virol. 81, 3058–3067.

Galluzzi, L., Pietrocola, F., Levine, B., Kroemer, G., 2014. Metabolic control of autophagy. Cell 159, 1263–1276.

Gannage, M., Dormann, D., Albrecht, R., Dengjel, J., Torossi, T., Ramer, P.C., Lee, M., Strowig, T., Arrey, F., Conenello, G., Pypaert, M., Andersen, J., Garcia-Sastre, A., Munz, C., 2009. Matrix protein 2 of influenza A virus blocks autophagosome fusion with lysosomes. Cell Host Microbe 6, 367–380.

Hahn, D.R., Na, C.L., Weaver, T.E., 2014. Reserve autophagic capacity in alveolar epithelia provides a replicative niche for influenza A virus. Am. J. Respir. Cell Mol. Biol. 51, 400–412.

Hale, B.G., Batty, I.H., Downes, C.P., Randall, R.E., 2008. Binding of influenza A virus NS1 protein to the inter-SH2 domain of p85 suggests a novel mechanism for phosphoinositide 3-kinase activation. J. Biol. Chem. 283, 1372–1380.

Hale, B.G., Jackson, D., Chen, Y.H., Lamb, R.A., Randall, R.E., 2006. Influenza A virus NS1 protein binds p85beta and activates phosphatidylinositol-3-kinase signaling. Proc. Natl. Acad. Sci. USA 103, 14194–14199.

He, L., Zhao, G., Zhong, L., Liu, Q., Duan, Z., Gu, M., Wang, X., Liu, X., Liu, X., 2013. Isolation and characterization of two H5N1 influenza viruses from swine in Jiangsu Province of China. Arch. Virol. 158, 2531–2541.

Herold, S., Ludwig, S., Pleschka, S., Wolff, T., 2012. Apoptosis signaling in influenza virus propagation, innate host defense, and lung injury. J. Leukoc. Biol. 92, 75–82.

Hrincius, E.R., Wixler, V., Wolff, T., Wagner, R., Ludwig, S., Ehrhardt, C., 2010. CRK adaptor protein expression is required for efficient replication of avian influenza A viruses and controls JNK-mediated apoptotic responses. Cell. Microbiol. 12, 831–843.

Hsu, A.C., 2018. Influenza Virus: a Master Tactician in Innate Immune Evasion and Novel Therapeutic Interventions. Front. Immunol. 9, 743.

Iwai, A., Shiozaki, T., Miyazaki, T., 2013. Relevance of signaling molecules for apoptosis induction on influenza A virus replication. Biochem Biophys. Res. Commun. 441, 531–537.

Kim, J., Kim, Y.C., Fang, C., Russell, R.C., Kim, J.H., Fan, W., Liu, R., Zhong, Q., Guan, K.L., 2013. Differential regulation of distinct Vps34 complexes by AMPK in nutrient stress and autophagy. Cell 152, 290–303.

Kim, J., Kundu, M., Viollet, B., Guan, K.L., 2011. AMPK and mTOR regulate autophagy through direct phosphorylation of Ulk1. Nat. Cell Biol. 13, 132–141.

Klein, S.R., Piya, S., Lu, Z., Xia, Y., Alonso, M.M., White, E.J., Wei, J., Gomez-Manzano, C., Jiang, H., Fueyo, J., 2015. C-Jun N-terminal kinases are required for oncolytic adenovirus-mediated autophagy. Oncogene 34, 5295–5301.

Klemm, C., Boergeling, Y., Ludwig, S., Ehrhardt, C., 2018. Immunomodulatory nonstructural proteins of influenza A viruses. Trends Microbiol. 26, 624–636.

Krug, R.M., 2015. Functions of the influenza A virus NS1 protein in antiviral defense. Curr. Opin. Virol. 12, 1–6.

Lai, S., Qin, Y., Cowling, B.J., Ren, X., Wardrop, N.A., Gilbert, M., Tsang, T.K., Wu, P., Feng, L., Jiang, H., Peng, Z., Zheng, J., Liao, Q., Li, S., Horby, P.W., Farrar, J.J., Gao, G.F., Tatem, A.J., Yu, H., 2016. Global epidemiology of avian influenza A H5N1 virus infection in humans, 1997–2015: a systematic review of individual case data. Lancet Infect. Dis. 16, e108–e118.

Li, W., Wang, G., Zhang, H., Shen, Y., Dai, J., Wu, L., Zhou, J., Jiang, Z., Li, K., 2012. Inability of NS1 protein from an H5N1 influenza virus to activate PI3K/Akt signaling pathway correlates to the enhanced virus replication upon PI3K inhibition. Vet. Res. 43, 36.

Li, Y., Anderson, D.H., Liu, Q., Zhou, Y., 2008. Mechanism of influenza A virus NS1 protein interaction with the p85beta, but not the p85alpha, subunit of phosphatidylinositol 3-kinase (PI3K) and up-regulation of PI3K activity. J. Biol. Chem. 283, 23397–23409.

Lindqvist, L.M., Frank, D., McArthur, K., Dite, T.A., Lazarou, M., Oakhill, J.S., Kile, B.T., Vaux, D.L., 2018. Autophagy induced during apoptosis degrades mitochondria and inhibits type I interferon secretion. Cell Death Differ. 25, 782–794.

Liu, G., Zhong, M., Guo, C., Komatsu, M., Xu, J., Wang, Y., Kitazato, K., 2016. Autophagy is involved in regulating influenza A virus RNA and protein synthesis associated with both modulation of Hsp90 induction and mTOR/p70S6K signaling pathway. Int. J. Biochem. Cell Biol. 72, 100–108.

Lu, X., Masic, A., Li, Y., Shin, Y., Liu, Q., Zhou, Y., 2010. The PI3K/Akt pathway inhibits influenza A virus-induced Bax-mediated apoptosis by negatively regulating the JNK pathway via ASK1. J. Gen. Virol. 91, 1439–1449.

Ludwig, S., Ehrhardt, C., Neumeier, E.R., Kracht, M., Rapp, U.R., Pleschka, S., 2001. Influenza virus-induced AP-1-dependent gene expression requires activation of the JNK signaling pathway. J. Biol. Chem. 276, 10990–10998.

Ludwig, S., Pleschka, S., Planz, O., Wolff, T., 2006. Ringing the alarm bells: signalling and apoptosis in influenza virus infected cells. Cell. Microbiol. 8, 375–386.

Ludwig, S., Wang, X., Ehrhardt, C., Zheng, H., Donelan, N., Planz, O., Pleschka, S., Garcia-Sastre, A., Heins, G., Wolff, T., 2002. The influenza A virus NS1 protein inhibits activation of Jun N-terminal kinase and AP-1 transcription factors. J. Virol. 76, 11166–11171.

Mack, H.I., Zheng, B., Asara, J.M., Thomas, S.M., 2012. AMPK-dependent phosphorylation of ULK1 regulates ATG9 localization. Autophagy 8, 1197–1214.

Munz, C., 2014. Influenza A virus lures autophagic protein LC3 to budding sites. Cell Host Microbe 15, 130–131.

Nacken, W., Anhlan, D., Hrincius, E.R., Mostafa, A., Wolff, T., Sadewasser, A., Pleschka, S., Ehrhardt, C., Ludwig, S., 2014. Activation of c-jun N-terminal kinase upon influenza A virus (IAV) infection is independent of pathogen-related receptors but dependent on amino acid sequence variations of IAV NS1. J. Virol. 88, 8843–8852.

Nacken, W., Ehrhardt, C., Ludwig, S., 2012. Small molecule inhibitors of the c-Jun N-terminal kinase (JNK) possess antiviral activity against highly pathogenic avian and human pandemic influenza A viruses. Biol. Chem. 393, 525–534.

Pan, H., Zhang, Y., Luo, Z., Li, P., Liu, L., Wang, C., Wang, H., Li, H., Ma, Y., 2014. Autophagy mediates avian influenza H5N1 pseudotyped particle-induced lung inflammation through NF-kappaB and p38 MAPK signaling pathways. Am. J. Physiol. Lung Cell Mol. Physiol. 306, L183–L195.

Perot, B.P., Boussier, J., Yatim, N., Rossman, J.S., Ingersoll, M.A., Albert, M.L., 2018. Autophagy diminishes the early interferon-beta response to influenza A virus resulting in differential expression of interferon-stimulated genes. Cell Death Dis. 9, 539.

Ren, Y., Li, C., Feng, L., Pan, W., Li, L., Wang, Q., Li, J., Li, N., Han, L., Zheng, X., Niu, X., Sun, C., Chen, L., 2015. Proton channel activity of influenza A virus matrix protein 2 contributes to autophagy arrest. J. Virol. 90, 591–598.

Rossman, J.S., Lamb, R.A., 2009. Autophagy, apoptosis, and the influenza virus M2 protein. Cell Host Microbe 6, 299–300.

Russell, R.C., Yuan, H.X., Guan, K.L., 2014. Autophagy regulation by nutrient signaling. Cell Res. 24, 42–57.

Shang, L., Chen, S., Du, F., Li, S., Zhao, L., Wang, X., 2011. Nutrient starvation elicits an acute autophagic response mediated by Ulk1 dephosphorylation and its subsequent dissociation from AMPK. Proc. Natl. Acad. Sci. USA 108, 4788–4793.

Shin, Y.K., Liu, Q., Tikoo, S.K., Babiuk, L.A., Zhou, Y., 2007a. Effect of the phosphatidylinositol 3-kinase/Akt pathway on influenza A virus propagation. J. Gen. Virol. 88, 942–950.

Shin, Y.K., Liu, Q., Tikoo, S.K., Babiuk, L.A., Zhou, Y., 2007b. Influenza A virus NS1 protein activates the phosphatidylinositol 3-kinase (PI3K)/Akt pathway by direct interaction with the p85 subunit of PI3K. J. Gen. Virol. 88, 13–18.

Siddiqui, M.A., Malathi, K., 2012. RNase L induces autophagy via c-Jun N-terminal kinase and double-stranded RNA-dependent protein kinase signaling pathways. J. Biol. Chem. 287, 43651–43664.

Steele, S., Brunton, J., Kawula, T., 2015. The role of autophagy in intracellular pathogen nutrient acquisition. Front. Cell. Infect. Microbiol. 5, 51.

Sun, Y., Li, C., Shu, Y., Ju, X., Zou, Z., Wang, H., Rao, S., Guo, F., Liu, H., Nan, W., Zhao, Y., Yan, Y., Tang, J., Zhao, C., Yang, P., Liu, K., Wang, S., Lu, H., Li, X., Tan, L., Gao, R., Song, J., Gao, X., Tian, X., Qin, Y., Xu, K.F., Li, D., Jin, N., Jiang, C., 2012. Inhibition of autophagy ameliorates acute lung injury caused by avian influenza A H5N1 infection. Sci. Signal 5, ra16.

Wei, Y., Pattingre, S., Sinha, S., Bassik, M., Levine, B., 2008a. JNK1-mediated phosphorylation of Bcl-2 regulates starvation-induced autophagy. Mol. Cell 30, 678–688.

Wei, Y., Sinha, S., Levine, B., 2008b. Dual role of JNK1-mediated phosphorylation of Bcl-2 in autophagy and apoptosis regulation. Autophagy 4, 949–951.

Wu, H.M., Wang, J., Zhang, B., Fang, L., Xu, K., Liu, R.Y., 2016. CpG-ODN promotes phagocytosis and autophagy through JNK/P38 signal pathway in Staphylococcus aureus-stimulated macrophage. Life Sci. 161, 51–59.

Xie, J., Zhang, S., Hu, Y., Li, D., Cui, J., Xue, J., Zhang, G., Khachigian, L.M., Wong, J., Sun, L., Wang, M., 2014. Regulatory roles of c-jun in H5N1 influenza virus replication and host inflammation. Biochim. Biophys. Acta 1842, 2479–2488.

Yeganeh, B., Ghavami, S., Kroeker, A.L., Mahood, T.H., Stelmack, G.L., Klonisch, T., Coombs, K.M., Halayko, A.J., 2015. Suppression of influenza A virus replication in human lung epithelial cells by noncytotoxic concentrations bafilomycin A1. Am. J. Physiol. Lung Cell Mol. Physiol. 308, L270–L286.

Zhang, D., Wang, W., Sun, X., Xu, D., Wang, C., Zhang, Q., Wang, H., Luo, W., Chen, Y., Chen, H., Liu, Z., 2016a. AMPK regulates autophagy by phosphorylating BECN1 at threonine 388. Autophagy 12, 1447–1459.

Zhang, S., Tian, H., Cui, J., Xiao, J., Wang, M., Hu, Y., 2016b. The c-Jun N-terminal kinase (JNK) is involved in H5N1 influenza A virus RNA and protein synthesis. Arch. Virol. 161, 345–351.

Zhang, P., Tang, Y., Liu, X., Peng, D., Liu, W., Liu, H., Lu, S., Liu, X., 2008. Characterization of H9N2 influenza viruses isolated from vaccinated flocks in an integrated broiler chicken operation in eastern China during a 5 year period (1998–2002). J. Gen. Virol. 89, 3102–3112.

Zhang, R., Chi, X., Wang, S., Qi, B., Yu, X., Chen, J.L., 2014. The regulation of autophagy by influenza A virus. Biomed. Res. Int. 2014, 498083.

Zhirnov, O.P., Klenk, H.D., 2013. Influenza A virus proteins NS1 and hemagglutinin along with M2 are involved in stimulation of autophagy in infected cells. J. Virol. 87, 13107–13114.

Zhong, L., Shu, W., Dai, W., Gao, B., Xiong, S., 2017. Reactive oxygen species-mediated c-Jun NH2-terminal kinase activation contributes to hepatitis B virus X protein-induced autophagy via regulation of the beclin-1/Bcl-2 interaction. J. Virol. 91.

Zhou, Z., Jiang, X., Liu, D., Fan, Z., Hu, X., Yan, J., Wang, M., Gao, G.F., 2009. Autophagy is involved in influenza A virus replication. Autophagy 5, 321–328.